15th Australasian Fluid Mechanics Conference
The University of Sydney, Sydney, Australia
13-17 December 2004

Further Study of Spray Combustion in a Simple Turbulent Jet Flow

Yung-Cheng Chen, Sten H. Stårner, and Assaad R. Masri

School of Aerospace, Mechanical & Mechatronic Engineering
The University of Sydney, NSW, 2006 AUSTRALIA

Abstract

A laboratory burner has been developed to study the combustion characteristics of dilute sprays dispersed in a turbulent round jet flow of air. The burner design is intended to extend previous work with piloted jet diffusion flames into turbulent combustion of spray jets. In this paper, the characteristics of a methanol spray flame are compared with those of an acetone spray flame and a non-reacting acetone spray jet. The Phase Doppler Anemometry technique is applied to measure droplet size, two-component velocity, number density and the axial volume flux. The results show that, when the droplet carrier is air, spray flames are premixed in nature with most of the droplets consumed in the vicinity of local flame fronts and have quite different droplet velocity profiles from those of the non-reacting spray jet.

Introduction

Spray combustion has a wide range of applications in power generation, including internal combustion engines and airborne propulsion. Its physical and chemical processes are made more complex by the largely unknown interactions between droplets, the turbulence, and chemical reactions involved. The capabilities of numerical predictions are often limited by the empiricism in the sub-models used for droplet evaporation, combustion and turbulence, and also by the lack of suitable experimental data for detailed comparison. A laboratory burner based on the spray jet configuration has been recently developed [1] to avoid some of the modelling difficulties often encountered in the near field, such as high initial velocity, flow recirculation, steep axial gradients, and non-uniform drop distribution. The well-defined boundary and initial conditions provided by this burner are particularly suitable for model validation purpose. Experimental data of this kind are very much needed by the spray combustion community [2].

The burner design extends the previous work with piloted jet diffusion flames [3] into turbulent combustion of spray jets. A nebulizer is placed upstream to generate droplets of different sizes, the distribution of which becomes fairly uniform at the burner exit. The slender shear flow field developed downstream is fluid mechanically well understood. Such flow fields are easily predicted with existing commercial CFD codes, so that the focus can be placed on evaporation and other aspects of droplet dynamics in turbulent spray flames. Similar burner design has also been used to investigate effects of the droplet-size distribution [4], burning modes of droplet clusters [5], and droplet/turbulence interactions [6,7].

Salient features of droplet dispersion and evaporation in non-reacting [1] and reacting [8] acetone spray jets generated by this burner have been reported recently. The aim of this work is to extend the current database to a different fuel and to investigate its effects on turbulent spray combustion. Methanol is chosen here because of the small difference in liquid density by less than 1%. It has also the same index of refraction at 1.36 as acetone, but a lower vapour pressure and a larger binary diffusion coefficient in air. This results in a longer evaporation time for methanol than acetone droplets of the same diameter for a single droplet in an infinite oxidizing environment.

The Phase Doppler anemometry (PDA) technique is applied to measure droplet size, two-component velocity, number density and the axial volume flux. The mean and rms velocities conditional on different size classes are compared for methanol and acetone spray flames. The differences in droplet dispersion between non-reacting and reacting sprays are also explored. Both the Sauter Mean Diameter (SMD) and the integrated liquid flux are then compared to reveal the controlling factors on the bulk fuel consumption rate.

Experimental Conditions

The schematic diagrams of the spray jet nozzle and burner are shown in Fig. 1. A co-flowing air stream at a mean velocity of 3 m/s and less than 2 per cent turbulence intensity is applied to shroud the spray jet and spray flame and to provide a well-defined boundary condition. The inner diameter of the main fuel tube, *D*, is the same at 9.8 mm. The main fuel tube is 75 mm long for the spray jet nozzle and is 50 mm long for the spray burner. Pressurized liquid fuel is fed into the nebulizer and its flow rate is measured by rotameters to be within 3% accuracy.

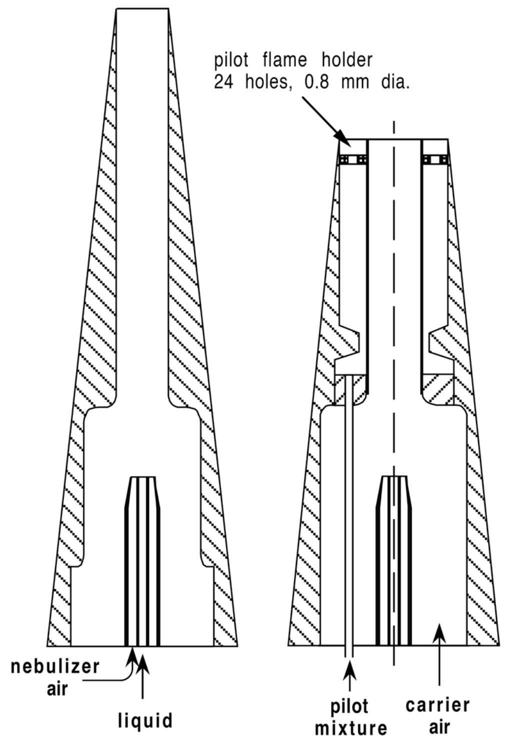

Figure 1: Spray jet nozzle (left) and burner (right) design.

On the thin burner lip, an annular premixed pilot flame anchors the spray flames. The pilot flame is a stoichiometric H_2/C_2H_2/air mixture such that the C/H ratio equals that of the main fuel, and its contribution to total heat release is 3.2 and 2.9 percent for flames MHF and AHF, respectively.

The global conditions for the methanol spray flame MHF, the acetone spray flame AHF, and the non-reacting spray jet LFS are listed in Table 1. The carrier air flow rate is maintained the same for both MHF and AHF flames to keep the jet Reynolds number the same.

	MHF	**AHF**	**LFS**
liquid fuel injected	methanol	acetone	acetone
liquid fuel injection rate (g/min)	26.3	21.1	7.0
carrier air flow rate (g/min)	170.4	170.4	135
overall fuel/air equivalence ratio	0.99	1.17	0.49
integrated vapour flux at nozzle exit (g/min)	-	11.4	5.9
gas-phase equivalence ratio at nozzle exit	-	0.63	0.41
D_{32} at nozzle exit (μm)	19.2	18.0	13.7
mean flame height (*x/D*)	15 ~ 20	15 ~ 20	

Table 1: Global operation conditions.

PDA measurements have been carried out that scan along the radial direction at several axial stations downstream until less than 5% of the injected fuel remains as liquid. Droplet diameters as well as the axial, *x*-, and radial, *r*-, components of droplet velocities are recorded with a PDA instrument (Aerometrics, RSA 3100) arranged in 45° forward scattering mode, with 3 micron fringe spacing. More details about the settings for the PDA system can be found in Ref. [8].

Results and Discussion

The thermal structure of methanol and acetone spray flames is first compared in Fig. 2. Mean flame temperature measured with a R-type thermocouple is shown at two axial stations. The bead diameter is approximately 0.2 mm. At the near burner exit location of $x/D = 5$, the methanol spray flame remains at ambient temperature close to the jet centreline; whereas the acetone flame is already at a higher temperature of approximately 300 ºC. The much lower temperature near the centreline for the methanol flame is attributed to both its longer droplet evaporation time and relatively higher liquid fuel injection rate. Substantial droplet evaporation is expected to occur at this axial station and reduces the gas phase temperature. Further downstream at $x/D = 15$ in the flame zone, the radial temperature profile becomes very similar for the methanol and acetone flames.

The centreline axial mean, $\bar{U}_{CL}$, and rms, u'_{CL}, velocities conditional on a particular size class are compared in Fig. 3 between the spray flame MHF and AHF. At axial locations of $x/D < 15$, both spray flames have almost the same droplet velocity for the same droplet size class. This indicates that response of droplet dispersion to turbulent convection is almost the same in both spray flames. Because the liquid density is the same for methanol and acetone, the droplet relaxation time is expected to be also the same for droplets of the same diameter.

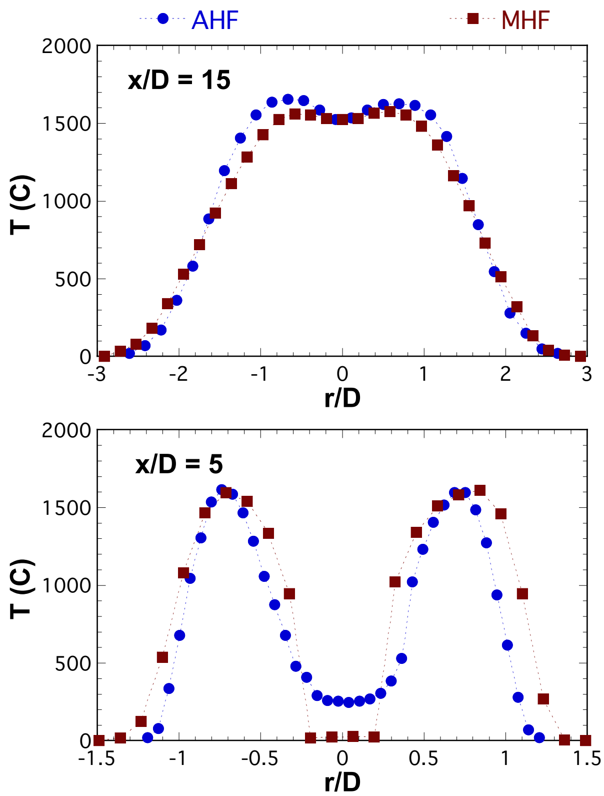

Figure 2: Comparison of the radial profiles of flame temperature at two axial stations for flames AHF and MHF.

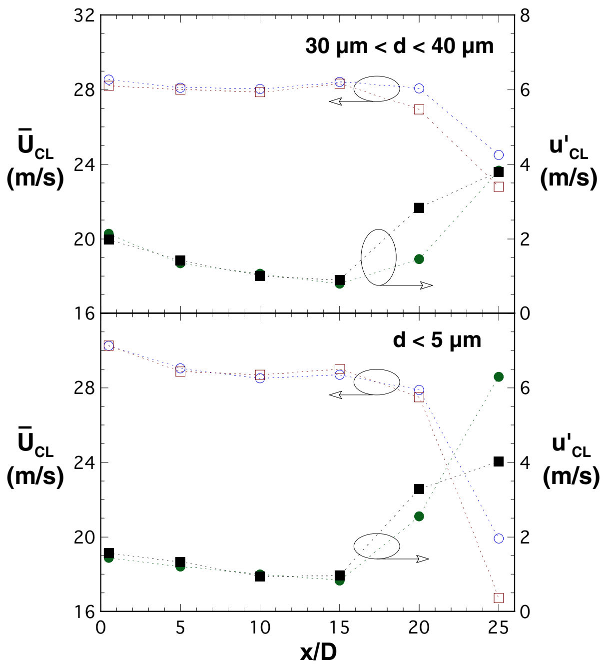

Figure 3: Comparison of the axial mean, $\bar{U}_{CL}$, and rms, u'_{CL}, velocities of droplets conditional on different size classes along the centreline for flame AHF: ○ and ●; and MHF: □ and ■. The open symbols represent the mean velocities and the closed symbols represent the rms velocities.

However, the methanol spray flame shows a faster decline of $\bar{U}_{CL}$ as well as the corresponding earlier rise of u'_{CL} than the acetone flame at axial stations of $x/D > 15$ for both small and large droplets. This is consistent with a slightly shorter flame length for flame MHF as is also observed in the faster rise of temperature along the centreline shown in Fig. 4. Despite a smaller droplet evaporation time, the longer acetone flame length is attributed to its slightly rich overall fuel/carrier air equivalence ratio of the jet, as seen in Table 1. The corresponding laminar burning velocity can be higher in the MHF than the AHF flame. This is related to the premixed-dominated nature for both spray jet flames investigated here.

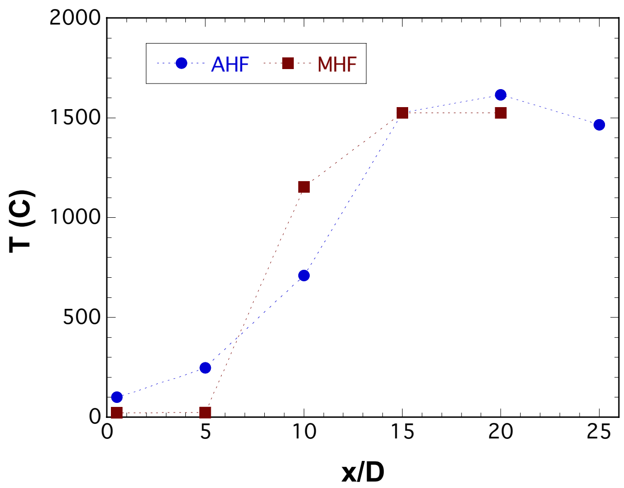

Figure 4. Comparison of the centreline flame temperature for flames AHF and MHF.

The droplet velocity distributions measured in non-reacting spray jets are quite different to those in the spray flames. Figure 5 compares the centreline axial mean and rms velocities of the spray jet LFS with the corresponding spray flame AHF. The axial mean velocity remains almost unchanged along the centreline up to $x/D = 20$ for the spray flames. In contrast, the decline of $\bar{U}_{CL}$ occurs already at axial locations of $x/D > 5$ for LFS in Fig. 5, indicating substantial droplet dispersion effects. The different trends for both $\bar{U}_{CL}$ and u'_{CL} are clearly associated with the much longer potential core in the spray flame than in the non-reacting counterpart. A similar extension of the potential core length has been observed before in turbulent premixed jet flames [9] where the turbulent flame brush is located at a smaller radius than the mixing layer, and thus retards the inward transport of turbulence generated at the mixing layer.

The resemblance to a premixed jet flame of the spray flames investigated here has been confirmed by OH-LIF imaging [10]. Almost all of the droplets are observed to evaporate within 1-2 mm of the local, instantaneous OH-fronts, irrespective of the fuel type. As the gas flow does not decay within the lengthened potential core, no apparent mean slip velocity is developed in the axial direction. Thus, the values of $\bar{U}_{CL}$ for droplets of all the size classes remain the same as the mean droplet velocity at the jet centreline for $x/D < 20$ in spray flames.

The droplet Sauter Mean Diameter (SMD), D_{32}, relative to that at the burner exit is compared in Fig 6 for flames AHF and MHF. The general behaviour of D_{32}, and the other mean droplet diameters as well, is the same for both flames. At a particular axial location, D_{32} remains almost constant in the jet core region and increases gradually towards the flame zone as small droplets are quickly consumed. Also, D_{32} increases monotonically along the axial direction. At the near burner exit axial station of $x/D = 5$, the relative SMD remains the same for both flames. This indicates that the difference in the droplet evaporation time and the liquid injection rate does not change substantially the mean droplet diameter.

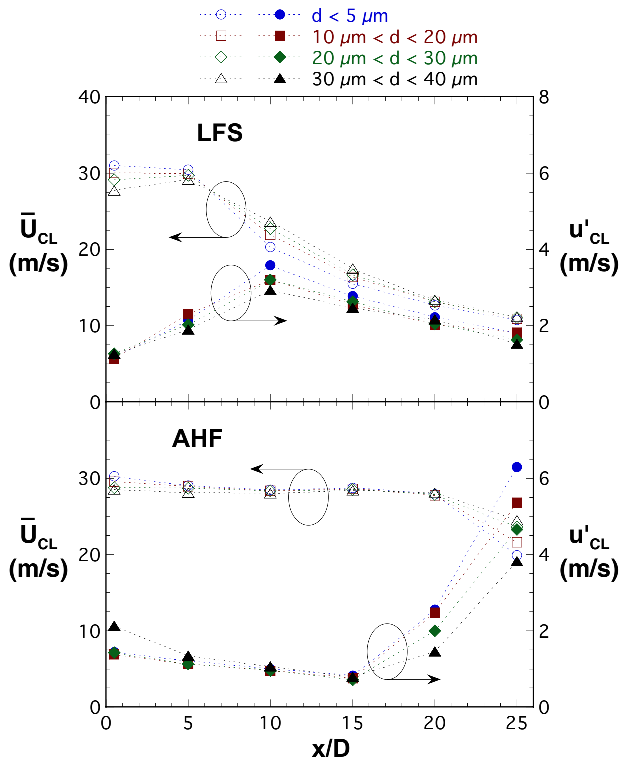

Figure 5: Comparison of the axial mean, $\bar{U}_{CL}$, and rms, u'_{CL}, velocities of droplets conditional on different size classes along the centreline for the non-reacting LFS spray jet and the reacting AHF spray flame. The open symbols represent the mean velocities and closed symbols represent the rms velocities.

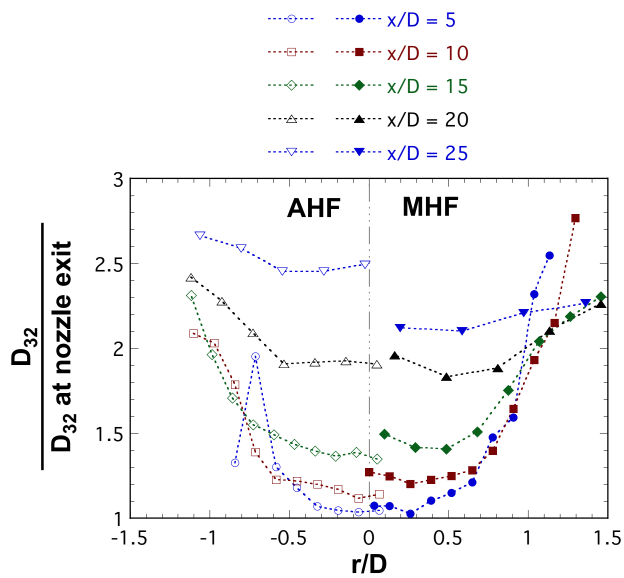

Figure 6: Comparison of the radial profiles of the Sauter mean diameter, D_{32}, at different axial stations for flames AHF and MHF.

Further downstream from x/D = 10 to x/D = 20, the mean droplet diameter is greater in the methanol flame than in the acetone flame in Fig. 6. This difference in the Sauter mean diameter suggests that small droplets are consumed faster in the former than the latter flame. This is counter-intuitive since, by vapour pressure consideration alone, acetone droplets are expected to evaporate faster than methanol. A higher burning velocity of the methanol flame than acetone flame may be responsible for the faster depletion of the small drops for the methanol spray jet. At the axial location of x/D = 25, higher Sauter mean diameter is found for the methanol spray jet and can be attributed to the faster evaporation of acetone droplets.

Compared with the acetone flame AHF, the methanol spray flame MHF has a higher fuel injection rate, but is slightly shorter in flame height. The flame zones are located at approximately the same radius at all axial stations judging from the temperature measurements. All these imply a faster bulk fuel consumption rate for the flame MHF. This is also supported by the integrated droplet mass flux plotted along the flight time, *t*, in Fig. 7. The flight time at a given axial location is obtained by integrating the reciprocal of the centreline mean axial velocity along the axis. A faster decline of the integrated droplet mass flux with time is found for spray flame MHF. Dashed lines in Fig. 7 indicate the erroneous PDA measurements at x/D = 0 and 10, where the liquid flux shows an unphysical increasing trend with increasing axial distance.

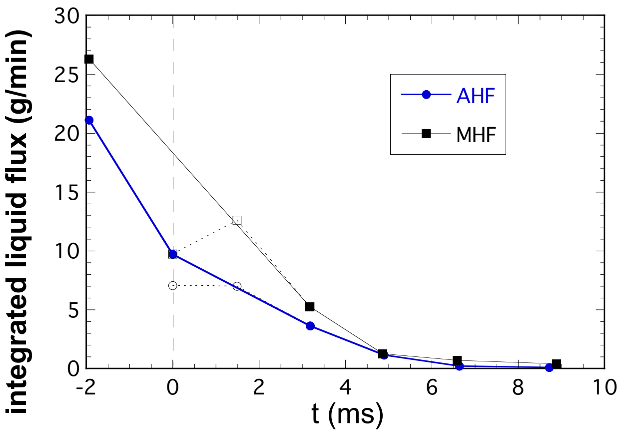

Figure 7: Comparison of the integrated liquid flux for flames AHF and MHF. Data points at x/D = 0 and 10 are plotted in open symbols to indicate that they may be susceptible to PDA measurement error.

Conclusions

The Phase Doppler Anemometry technique is applied to measure the droplet size, two-component velocity, and the axial volume flux in a methanol spray flame. Comparison is also made with an acetone flame and a non-reacting acetone spray jet. Despite the longer droplet evaporation time and higher liquid fuel injection rate for methanol than acetone flame, the methanol spray flame shows a faster bulk fuel consumption rate. This indicates that the premixed flame nature dominates the droplet evaporation process, which occurs mostly in the vicinity of the local flame front.

The premixed flame nature also affects strongly the droplet velocity profiles in the spray flames in comparison with those measured in the non-reacting spray jets. The axial mean velocity remains almost the same along the axial axis until reaching the flame tip near x/D = 20. Droplet dispersion and its interactions with the mixing layer are substantially suppressed in the spray flames than in non-reacting jet flows.

Acknowledgments

This work is supported by the Australian Research Council.

References

[1] Chen, Y.-C., Stårner, S.H., & Masri, A.R., Combined PDA/LIF Measurements in Simple, Evaporating Turbulent Spray Jets, in *Proceedings of the Fourteenth Australasian Fluid Mechanics Conference*, Adelaide, Australia, 2001, 267-270.

[2] Widmann, J.F. & Presser, C., A Benchmark Experimental Database for Multiphase Combustion Model Input and Validation, *Combust. Flame* **129**, 2002, 47-86.

[3] Bilger, R.W., Advanced Laser Diagnostics: Implications of Recent Results for Advanced Combustor Models, in *Aerothermodynamics in Combustors*, editors R.S.L. Lee, J.H. Whitelaw and T.S. Wung, Springer-Verlag, Heidelberg, 1992, 3-16.

[4] Bossard, J.A. & Peck, R.E., Droplet Size Distribution Effects in Spray Combustion, *Proc. Combust. Inst.* **26**, 1996, 1671-1677.

[5] Akamatsu, F., Mizutani, Y., Katsuki, M., Tsushima, S., Cho, Y.D., & Nakabe, K., Group Combustion Behavior of Droplets in a Premixed-Spray Flame, *Atomization and Sprays*, **7**, 1997, 199-218.

[6] Karpetis, A.N. & Gomez, A., Self-Similarity, Momentum Scaling and Reynolds Stress in Non-Premixed Turbulent Spray Flames, *J. Fluid Mech.* **397**, 1999, 231-258.

[7] Sornek, R.J., Dobashi, R., & Hirano, T., Effects of Turbulence on Dispersion and Vaporization of Droplets in Spray Combustion, *Proc. Combust. Inst.* **28**, 2000, 1055-1062.

[8] Chen, Y.-C., Stårner, S.H., & Masri, A.R., Characteristics of Turbulent Spray Combustion in a Piloted Jet Flame Burner, *Proc. Combust. Inst.* **29**, 2002, 625-632.

[9] Chen, Y.-C., Peters, N., Schneemann, G.A., Wruck, N., Renz, U., & Mansour, M.S., The Detailed Flame Structure of Highly Stretched Turbulent Premixed Methane-Air Flames, *Combust. Flame* **107**, 1996, 223-244.

[10] Stårner, S.H. & Masri, A.R., Mass Flux Measurements in Simple, Evaporating Turbulent Spray Jets, in *Proceedings of the Third Australian Conference on Laser Diagnostics in Fluid Mechanics and Combustion*, Brisbane, Australia, 2002, 114.